Fullerenes, Nanotubes and Carbon Nanostructures

ISSN: (Print) (Online) Journal homepage: https://www.tandfonline.com/loi/lfnn20

Simulation of fullerene formation in a carbon-helium plasma

Pavel V. Novikov, Irina V. Osipova, Grigory N. Churilov & Alexander I. Dudnik

To cite this article: Pavel V. Novikov, Irina V. Osipova, Grigory N. Churilov & Alexander I. Dudnik (2021) Simulation of fullerene formation in a carbon-helium plasma, Fullerenes, Nanotubes and Carbon Nanostructures, 29:5, 337-342, DOI: 10.1080/1536383X.2020.1842738

To link to this article: https://doi.org/10.1080/1536383X.2020.1842738

Published online: 06 Nov 2020.

FULLERENES, NANOTUBES AND CARBON NANOSTRUCTURES
2021, VOL. 29, NO. 5, 337–342
https://doi.org/10.1080/1536383X.2020.1842738

Simulation of fullerene formation in a carbon-helium plasma

Pavel V. Novikov[a], Irina V. Osipova[b], Grigory N. Churilov[b,c], and Alexander I. Dudnik[b,c]

[a]Krasnoyarsk Institute of Railway Transport, Krasnoyarsk, Russia; [b]Kirensky Institute of Physics, Federal Research Center KSC SB RAS, Krasnoyarsk, Russia; [c]Siberian Federal University, Krasnoyarsk, Russia

ABSTRACT

A kinetic model of fullerene formation in the carbon-helium plasma of an arc discharge was proposed. In the model, in addition to the coagulation of carbon clusters, the cluster isomerization and their cooling with a buffer gas were taken into account. The simulation results of the fullerene formation are in qualitatively agreement with the experimental data, i.e., the fraction of higher fullerenes increases at high pressures in the fullerene mixture.

ARTICLE HISTORY
Received 17 October 2020
Accepted 23 October 2020

KEYWORDS
Fullerene formation; kinetic model; carbon clusters

1. Introduction

In 1985, a new allotropic modification of carbon, i.e., the fullerene molecule C_{60} being a closed spherical shell was first obtained. Subsequently, the fullerenes C_{70} and higher (C_{76}, C_{78}, C_{80}, C_{84} and others) were obtained. When the synthesis method of fullerenes using an arc discharge between graphite electrodes in a helium atmosphere was discovered,[1] it became possible for the fullerenes C_{60} and C_{70} in gram quantities to be obtained. To develop some efficient method for fullerene synthesis, the simulation concepts of fullerene formation mechanisms in the arc - discharge plasma is of great interest. Currently the fullerene formation mechanisms haven't been fully studied. The present models describe the fullerene formation as an assembly of smaller carbon clusters, neutral[2–4] or charged,[5] as well as annealing of large fullerenes with the loss of C_2 dimers.[6] Since the formation of fullerenes occurs under nonequilibrium conditions, the yield of fullerenes can be affected by changing the temperature gradient in the carbon-helium plasma. The main influence on the temperature gradient in the arc discharge is exerted by the arc current[7] and the buffer gas pressure.[8,9] In,[7] the influence of the acoustic field on the yield of fullerenes was also experimentally shown, probably due to gas-dynamic resonance phenomena in the reaction chamber. In addition, the temperature gradient can be affected by the rotation of the buffer gas or by the rotating co-phase magnetic field.

The calculation results of the fullerene formation in carbon-helium plasma at different buffer gas pressures based on the kinetic model given below were presented.

2. Coagulation model of carbon clusters when cooled by a buffer gas

The fullerene formation takes place at the periphery of the arc discharge during cooling of the carbon-helium plasma in the range from 3500 K to 2000 K.[10]

In an arc discharge, carbon vapor in helium serves as a small additive. In the hot region of the arc discharge, there are only carbon C_2 dimers, assembling carbon clusters from those, including fullerenes. Different-shaped clusters with unsaturated radicals coagulate, to form soot particles or fullerenes upon cooling, with irregular particles doing soot. Being a part of soot, fullerenes remain isolated molecules, which can be further isolated by non-polar solvents. Their mass fraction can be 5–15% of the soot obtained.

When the carbon clusters collide with each other, new ones are formed and then continue to transform by the emergence of new bonds between atoms. When forming each bond, an energy within the order of several electron volts is released, which is then distributed over the vibrational degrees of freedom of the cluster. In that case, the vibrational temperature increase of a cluster can lead to its reverse decay into smaller clusters. Therefore, the stable process of cluster coagulation is directly associated with their cooling in collisions with buffer gas atoms.[11]

The paper discusses the results of solving the kinetic equations of reactions and carbon cluster transformation. Since the number of possible clusters and reactions between them is enormous, several simplifications have been adopted. A similar scheme for an abbreviated description of the kinetics of carbon cluster coagulation was first proposed in ref.[12,13]

As the number of even carbon clusters in the arc discharge plasma is much higher than the number of odd clusters according to the mass spectroscopic analysis,[14] these are clusters with an even atom number which were used in all calculations. The clusters with the number of atoms k from two to 120 were taken into account. From this perspective, the C_{120} cluster concentration should be construed as the concentration of all clusters and soot particles with at least 120 atoms.

It is known that the best structure of small carbon clusters condensing in the arc discharge plasma is known to be

CONTACT Pavel V. Novikov novikov_pv@krsk.irgups.ru Krasnoyarsk Institute of Railway Transport, Krasnoyarsk, Russia.

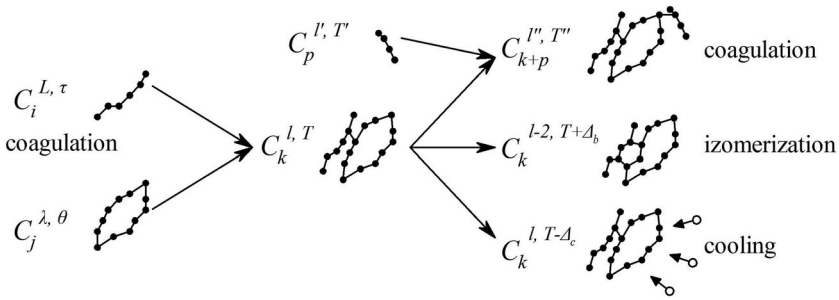

Figure 1. A schematic diagram of reactions in which the carbon clusters $C_k^{l,T}$ including the carbon atoms k, having the radical bonds l and a vibrational temperature T are formed or disappear. Carbon atoms are depicted by black, buffer gas atoms are white.

those with sp- or sp^2- hybridization of carbon atoms, i.e., chains, rings, pieces of single-layer graphite (graphene) planes and their combinations.[15] Therefore, as assumed in the model, carbon atoms in a cluster can have a maximum of two radicals.

Thus, monocyclic clusters with $k = 10 - 20$ will have one radical per atom ($l = k$), carbon chains with $k = 2 \ldots 16$ will have one more radical at the ends, i.e., therefore $l = k + 2$. Clusters of different structures with the number of atoms $k \geq 20$ can have a different number of radicals: $l \in [l_{\min};\ l_{\max}]$, depending on k. Fullerene molecules will differ from other clusters by the absence of radicals: $l = 0$.

It was specified in the model that only carbon clusters C_{60}, C_{70}, C_{78} and C_{84} can be fullerenes. Since higher fullerenes C_n with $n > 70$ are experimentally formed in significantly smaller amounts than C_{60} and C_{70}, only C_{78} and C_{84} were taken into account to reveal only the fundamental features of the higher fullerene formation under different synthesis conditions.

Let us introduce a notation $C_k^{l,T}$ for a carbon cluster C_k, where l is radical bonds and T is vibrational temperature. The concentration of clusters $C_k^{l,T}$ in a carbon-helium plasma is denoted as $n(k, l, T)$. While solving the kinetic equations at each time step, the concentration distribution of carbon clusters $n(k, l, T)$ over k, l and T was calculated in some unit volume, where the temperature decreases at the rate of the volume removal from the discharge axis ~ 20 m/s. A schematic diagram of reactions, where a carbon cluster is a reagent or product, is shown in Figure 1.

An increase in the cluster concentration C_k s occurs as a result of coagulation of smaller clusters C_i and C_j with the number of atoms $i + j = k$, with the number of radical bonds L and λ and vibrational temperatures τ and θ, respectively:

$$C_i^{L,\tau} + C_j^{\lambda,\theta} \rightarrow C_k^{l,T} \tag{1}$$

In this case, the concentration of the C_k cluster decreases in the similar fusion reactions with other C_p clusters with an appropriate number $p = 2 \ldots 120$.

As supposed in the model one new bond is formed at the moment of collision of the C_i and C_j clusters. In other words, the newly formed C_k cluster has the number of radical bonds $l = L + \lambda - 2$. The temperature of the merged cluster immediately after fuzing the two clusters was set as $T = (i\tau + j\theta)/k$.

The process rates were set using the reaction constants $K_{i,j}^{L,\lambda}$.

It was assumed that then the isomerization process takes place, i.e., the number of radicals decreases due to the bonding of carbon atoms to each other, with the energy released in this process distributed over the vibrational degrees of freedom of the cluster:

$$C_k^{l,T} \rightarrow C_k^{l-2,\quad T+\Delta_b}, \tag{2}$$

where Δ_b is the increment in the vibrational temperature of the cluster when one bond is formed. The rates of these processes were set by the reaction constants M_k^l.

In addition, there was assumed to be an equalization of the vibrational temperatures of the clusters and the buffer gas temperature. If the cluster temperature T is lower than the buffer gas temperature, it heats up, in the opposite case, it cools down:

$$C_k^{l,T} \rightarrow C_k^{l,\quad T-\Delta_c}, \tag{3}$$

where Δ_c is the change in the vibrational temperature of the cluster due to collisions with the buffer gas atoms. The cooling / heating rates of the clusters were described by the reaction constants N_k^l.

In the current work, a system of kinetic equations was calculated as:

$$\begin{aligned}\frac{d}{dt}n(k,l,T) = &\sum_{\substack{i+j=k \\ L+\lambda-2=l}} K_{i,j}^{L,\lambda} \cdot n(i,L,\tau) \cdot n(j,\lambda,\theta) \\ &- \sum_{p \leq 120} K_{k,p}^{l,l'} \cdot n(k,l,T) \cdot n(p,l',T') - \\ &- M_k^l \cdot n(k,l,T) + M_k^{l+2} \cdot n(k,l+2,T-\Delta_b) - N_k^l \cdot n(k,l,T) \\ &+ N_k^l \cdot n(k,l,T+\Delta_c),\end{aligned} \tag{4}$$

where the first term describes the increase in the concentration $n(k, l, T)$ of the $C_k^{l,T}$ cluster using all possible reactions (1), the second one represents the decrease in the cluster concentration in all possible reactions $C_k^{l,T} + C_p^{l',T'} \rightarrow C_{k+p}^{l'',T''}$. The third and fourth terms do the decrease and increase in the $C_k^{l,T}$ cluster concentration due to the formation of new bonds in the cluster. The fifth and sixth terms do the decrease and increase in the $C_k^{l,T}$ cluster concentration due to cooling or heating in collisions with a buffer gas. A schematic diagram of the reactions of a carbon cluster is shown in Figure 1.

The reaction constants were calculated as follows:

$$K_{i,j}^{L,\lambda} = \sigma_{i,j}^{L,\lambda} \cdot P_{i,j} \cdot \mathrm{v}_{i,j} \cdot P_b \tag{5}$$

where $\mathrm{v}_{i,j} = \sqrt{8T/\pi\mu_{i,j}}$ is the average relative speed of two clusters; $\mu_{i,j} = m_i m_j/(m_i + m_j)$ – the relative mass of the C_i and C_j clusters; $\sigma_{i,j}^{L,\lambda}$ is the geometrical cross-section of the collisions of two clusters, depending on the number of radical bonds in both clusters: $\sigma_{i,j}^{L,\lambda} = \pi r_b^2 L\lambda$, where r_b is the effective radius where radical bonds can merge, i.e., both clusters can join each other only in those sites where there are some radicals. The value r_b= 1.7 Å was used in the calculations;

$P_b = \exp(-E_{ab}/T_g)$ is the probability of overcoming the activation barrier E_{ab} of merging two clusters. Due to the great complexity of calculating E_{ab} for all clusters, the average value E_{ab}= 2.0 eV, given in ref.[16] was used in the calculations.

Earlier, the presence of charged particles in carbon-helium plasma was first shown to have a significant effect on the rate of coagulation of carbon clusters.[5,17] Therefore, the cross section for collisions of neutral particles $\sigma_{i,j}^{L,\lambda}$ in the calculations was multiplied by the factor $P_{i,j}$, which depends on the charges of the colliding clusters.

According to the theory of charged particle collisions,[18] if the C_i and C_j clusters have charges q_i and q_j, respectively, the cross-section for collisions of neutral particles $\sigma_{i,j}^{L,\lambda}$ will be multiplied by the factor $P_{i,j}$:

$$P_{i,j} = \sum_{q_i=-2}^{+1} \sum_{q_j=-2}^{+1} \left(1 - \frac{q_i q_j \cdot p_i p_j}{\varepsilon_{\mathrm{kin}} \cdot (r_i + r_j)}\right), \tag{6}$$

where $r_i + r_j$ is the sum of the effective radii of both clusters, which determines the minimum distance between them; $\varepsilon_{kin} = 3/2 \cdot T$ is the average kinetic energy of the relative motion of both clusters; $p_i(q_i)$ and $p_j(q_j)$ are the probabilities that both clusters will have charges q_i и q_j. These probabilities were determined for each cluster using the Saha equations.[19]

In the calculations, only the most expectable charges $q_k = \{-2, -1, 0, 1\}$ for all clusters C_k were considered. To take into account the charges, the values of the ionization potential and electron affinity were calculated in the VASP package[20] for some carbon clusters and then interpolated for clusters of all sizes for $k = 2 \div 120$.

The rate constant for the formation of new bonds in a cluster was calculated as follows:[21]

$$M_k^l = \nu_{ph} \exp(-E_b/T_{vib}), \tag{7}$$

where T_{vib} is the vibrational temperature of the cluster; $E_b \approx 2.0$ eV is the barrier for the formation of a new chemical bond in the cluster; $\nu_{\mathrm{ph}} = 1011\mathrm{s}^{-1}$ is the effective frequency of atomic vibrations in a carbon cluster, calculated by averaging these frequencies for different carbon clusters.

The rate constant of the processes of cooling the cluster by the buffer gas was calculated as follows:

$$N_k^l = \frac{dT_k}{dt} \cdot \frac{\Delta t}{\Delta T}, \tag{8}$$

where dT_k/dt is the rate of cooling of the cluster C_k by the buffer gas, $\Delta t = 10^{-9}...10^{-8}$s is the time integration step of the differential equation system, and $\Delta T = 200$ K is sampling interval of the vibrational cluster temperature. According to the calculation results, the range of the cluster temperature distribution was determined from 2000 to 6000 K.

The vibrational temperature of the C_k cluster was considered to change at a rate

$$dT_k/dt = \langle \Delta E \cdot \mathrm{V}_g \rangle n_g \sigma_g, \tag{9}$$

where ΔE is the kinetic energy change of a helium atom upon collision with a carbon cluster, n_g is the concentration of helium; V_g is the velocity of the relative motion of the helium atom and the cluster; $\sigma_{k,g} = \pi(r_k + r_g)^2$ is their collision cross section, where r_k and r_g are the effective radii of the C_k cluster and the helium atom, respectively. Averaging was carried out over the Maxwellian distribution of the velocity of helium atoms.

The kinetic energy change of a helium atom when colliding with a carbon cluster:

$$\langle \Delta E \rangle = m_g \langle \Delta {V_g}^2 \rangle / 2 \tag{10}$$

where $\langle \Delta {V_g}^2 \rangle = \langle V_g^2 - (V'_g)^2 \rangle$ is the change in the velocity squared of the helium atom before and after the collision V_g and V'_g averaged over the Maxwellian distribution of the velocities of the helium atoms. The velocity of a helium atom after an elastic collision with a carbon atom in the C_k cluster is following

$$V'_g = \frac{(m_{k,g} - m_k) \cdot V_g + 2 m_k V_{eff}}{m_k + m_{He}} \tag{11}$$

where $V_{eff} = \pm V_{He} \pm V_C$ is the relative velocity of the helium and carbon atoms in the cluster. In a collision, the total velocity of the carbon atom can be estimated as $V_C = V_k \pm V_{vib}$, where $V_k = \sqrt{k_B T/m_k}$ is the average velocity of cluster displacement C_k, k_B is the Boltzmann constant, and $V_{vib} = \sqrt{1/3 \cdot E_{vib}/m_C}$ is the reference velocity of vibrations of the cluster walls, where

$$E_{vib} = \frac{3k - 6}{k} \cdot \frac{k_B T}{2} \tag{12}$$

is the average vibrational energy of the cluster per atom, where (3*k*–6) is the number of degrees of freedom of the C_k cluster.

In the calculation, when the plasma moves away from the arc axis, the temperature gradient was given by the formula

$$T \sim T_0 \cdot r^{-\alpha}, \tag{13}$$

where r is the distance from the center of the arc, and T_0 and α are empirical parameters.[22]

The empirical parameters for different pressures were selected so as formula (13) extrapolated the experimental dependence of the plasma temperature on the distance to the arc axis.[8]

To carry out the calculations, the program code was written with the GNU Fortran 90 language.

Table 1. The content of individual fullerenes in relation to the total content of fullerenes in soot at different pressures.[8]

P, kPa	The total yield of the fullerene mixture S_{full}, wt.%	Fullerene fraction in the mixture S_n/S_{full}, %		
		C_{60}	C_{70}	C_n ($n > 70$)
82.6	7.0	75.4	19.8	4.2
353	7.0	59.0	24.6	16.4

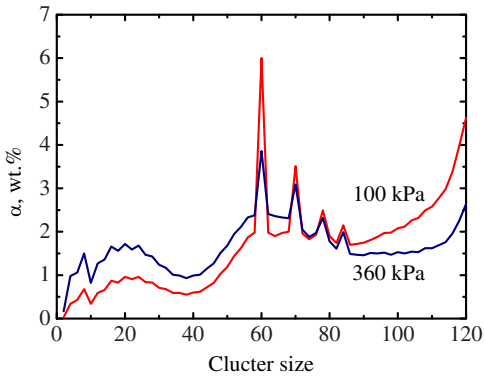

Figure 2. Calculated carbon cluster mass distribution at different pressures 75 μs after the start of reactions.

Table 2. Calculation results.

P, kPa	The total yield of the fullerene mixture S_{full}, wt.%	Fullerene fraction in the mixture S_n/S_{full}, %		
		C_{60}	C_{70}	C_n, $n > 70$
100	14.1	42	25	33
360	11.3	34	27	39

3. Results and discussion

It has previously been carried out some experiments on the fullerene synthesis in the plasma of a high-frequency arc discharge at various pressures:[8] from 13.3 to 353 kPa. The results of fullerene extraction have shown that the yield of higher fullerenes increases at high pressure. The values of the yield of fullerenes C_{60}, C_{70} and higher as a percentage of the total yield of fullerenes at two different helium pressures are given in Table 1.

In the current work, the fullerene formation at pressures of 100 kPa and 360 kPa for 75 μs, corresponding to the cooling of the carbon-helium plasma in the temperature range from 3200 to 2200 K during expansion from the axis of the arc discharge has been simulated. During this time, the coagulation and annealing of carbon clusters occur almost completely. Upon completing the calculation the final distribution of carbon clusters at various pressures is shown in Figure 2. At low pressure, more large clusters with a mass of 60 atoms or more are formed; and finally their fraction was 75%, and 60% at high pressure. Differences in the accumulation of large clusters lead to a different ratio of fullerenes in the mixture with a change in pressure.

The total yield of fullerenes and the percentage in the mixture is given in Table 2. The percentage of higher fullerenes with $n > 70$ is represented by the sum of the mass fractions of the C_{78} and C_{84} fullerenes. As it follows from the table that the calculation results are in qualitative agreement

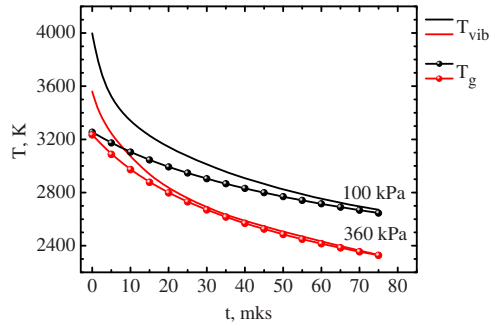

Figure 3. Time dependence of the buffer gas temperature T_g and the average vibrational cluster temperature T_{vib} with the number of atoms from 30 to 120.

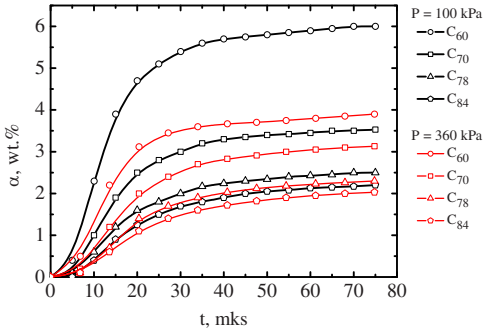

Figure 4. Change in the mass fraction of fullerenes for different pressures. At 100 kPa is depicted with black color, at 360 kPa is with red one.

with the experimental results, i.e., the percentage of higher fullerenes is higher at high pressure, with the C_{60} fullerene being lower.

The difference in the number of large clusters, including fullerenes, can be accounted for by the different condition of cluster cooling with a buffer gas. The time dependences of the buffer gas temperature and the average vibrational temperature of large clusters with a number of atoms from 30 to 120 are given in Figure 3. At low pressure, when moving away from discharge axis the temperature gradient is smaller, the gas temperature T_g is on average higher than at high pressure, which leads to an acceleration of coagulation reactions, and therefore the accumulation of large clusters. Also, a high vibrational temperature is maintained longer for carbon clusters at low pressure of buffer gas, which leads to an acceleration of the isomerization process toward an increase in the number of cluster bonds, and hence to that of the fullerene accumulation. The graphs of changes in the mass fraction of fullerenes at two different pressures are represented in Figure 4. As it follows from the graphs that most of fullerenes are formed in the first 20–30 μs from the beginning of the carbon cluster coagulation. This is due to the larger difference between the vibrational cluster temperature and the gas temperature at the beginning of the process (Figure 3). The result is consistent with experimental data and calculations of other authors.[13]

The processes of coagulation, cooling, and isomerization of carbon clusters are illustrated in more detail using the cluster distribution by the number of radicals and vibrational temperatures. The distribution of the cluster concentration C_{60} for an intermediate time point $t = 40$ μs for a pressure of 100 kPa is given in Figure 5. The most active

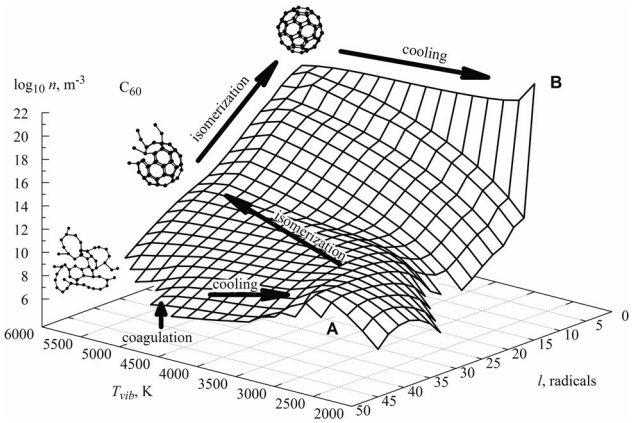

Figure 5. Cluster concentrations C_{60} with different numbers of radicals and different vibrational temperatures. The principal routes for the cluster transformation C_{60} into fullerene are shown with the arrows.

coagulation occurs in clusters with a large number of radicals, then they are cooled to the gas temperature, resulting in a local maximum A of the cluster concentration C_{60} with a large number of radicals. With further isomerization, the vibrational cluster temperature increases and, at the same time, the number of radicals decreases to zero, therefore the result of isomerization turns out to be a fullerene. Then, the fullerene molecules are cooled and accumulated at a temperature equal to the buffer gas temperature (point B). Under various conditions for the fullerene synthesis, their yield is determined by the ratio of the cluster concentrations C_{60} at points A and B. For "non-fullerene" clusters with a different number of atoms, the processes differ in that the final clusters have 2–4 radicals, which means that they participate in further reactions and the concentration does not increase as sharply as the concentration of fullerenes.

The distribution of the cluster concentration C_{60} will be similar at 360 kPa, with the concentration of incomplete clusters (point A) being higher, and the concentration of fullerenes (point B) being lower.

A larger number of higher fullerenes at high pressure can be due to the fact that clusters not having time to form the fullerene C_{60}, create higher fullerenes.

4. Conclusion

A kinetic model of carbon cluster coagulation in carbon-containing plasma was developed, taking into account the processes of heating or cooling of the cluster when forming a chemical bond and during colliding with buffer gas. Kinetic calculations have shown that the efficiency of fullerene formation depends on the rate of cooling of the carbon cluster during coagulation. The calculations have been qualitatively simulated the experimental results[8,9] in which the yield of higher fullerenes increases at high pressure of buffer gas. The influence of the arc discharge and the acoustic and magnetic fields[7] can be accounted in the further magnetohydrodynamic analysis of arc discharge conditions. Also, the further development of the model taking into account the dissociation model of giant fullerenes[6] can provide a more accurate distribution of various fullerenes in the resulting mixture and develop the controlled synthesis methods of higher fullerenes.

Disclosure statement

The authors declare that they have no conflict of interest.

Funding

The reported study was funded by RFBR according to the research project № 18-32-20011.

References

[1] Krätschmer, W.; Lamb, L. D.; Fostiropoulos, K.; Huffman, D. R. Solid C_{60}: A New Form of Carbon. *Nature* **1990**, *347*, 354–358. DOI: 10.1038/347354a0.

[2] Von Helden, G.; Gotts, N. G.; Bowers, M. T. Experimental Evidence for the Formation of Fullerenes by Collisional Heating of Carbon Rings in the Gas Phase. *Nature* **1993**, *363*, 60–63. DOI: 10.1038/363060a0.

[3] Heath, J. R. *Fullerenes: Synthesis, Properties and Chemistry of Large Carbon Clusters*; Hammond, G. S.; Kuck, V. J., Eds. American Chemical Society: Washington, DC, **1991**; pp 1–23.

[4] Hernández, E.; Ordejón, P.; Terrones, H. Fullerene Growth and the Role of Nonclassical Isomers. *Phys. Rev. B.* **2001**, *63*, 193403–1934034. DOI: 10.1103/PhysRevB.63.193403.

[5] Churilov, G. N.; Fedorov, A. S.; Novikov, P. V. Influence of Electron Concentration and Temperature on Fullerene Formation in a Carbon Plasma. *Carbon* **2003**, *41*, 173–178. DOI: 10.1016/S0008-6223(02)00276-2.

[6] Irle, S.; Zheng, G.; Wang, G.; Morokuma, K. The C_{60} Formation Puzzle "Solved": QM/MD Simulations Reveal the Shrinking Hot Giant Road of the Dynamic Fullerene Self-Assembly mechanism. J. Phys. Chem. B. **2006**, *110*, 14531–14545. DOI: 10.1021/jp061173z.

[7] Churilov, G. N. Synthesis of Fullerenes and Other Nanomaterials in Arc Discharge. *Fullerenes NanotubesCarbon Nanostruct.* **2008**, *16*, 395–403. DOI: 10.1080/15363830802281641.

[8] Churilov, G. N.; Krätschmer, W.; Osipova, I. V.; Glushenko, G. A.; Vnukova, N. G.; Kolonenko, A. L.; Dudnik, A. I. Synthesis of Fullerenes in a High-Frequency Arc Plasma under Elevated Helium Pressure. *Carbon* **2013**, *62*, 389–392. DOI: 10.1016/j.carbon.2013.06.022.

[9] Dudnik, A. I.; Osipova, I. V.; Nikolaev, N. S.; Churilov, G. N. Comparative Analysis of Two Methods for Synthesis of Fullerenes at Different Helium Pressures. *Fuller. Nanotub. Car. N.* **2020**, *28*, 697–701. DOI: 10.1080/1536383X.2020.1746281.

[10] Huczko, A.; Lange, H.; Byszewski, P.; Poplawska, M.; Starski, A. Fullerene Formation in Carbon Arc: Electrode Gap Dependence and Plasma Spectroscopy. *J. Phys. Chem. A.* **1997**, *101*, 1267–1269. DOI: 10.1021/jp962714v.

[11] Fedorov, A. S.; Novikov, P. V.; Martinez, Y. S.; Churilov, G. N. Influence of Buffer Gas and Vibration Temperature of Carbon Clusters on Fullerene Formation in a Carbon Plasma. J. *Nanosci. Nanotechnol.* **2007**, *7*, 1315–1320. DOI: 10.1166/jnn.2007.309.

[12] Alekseev, N. I.; Dyuzhev, G. A. Production of Fullerenes in Gas Discharge Plasmas. I. Kinetics of Fullerene Formation from Polycyclic Structures. *Tech. Phys.* **1999**, *44*, 1093–1097. DOI: 10.1134/1.1259479.

[13] Alekseev, N. I.; Dyuzhev, G. A. A Statistical Model of Fullerene Formation Based on Quantum Mechanical Calculations. II. Verification of the Model and Kinetics of Transformation into

Fullerene. *Tech. Phys.* **2001**, *46*, 577–583. DOI: 10.1134/1.1372949.

[14] Cox, D. M.; Reichmann, K. C.; Kaldor, A. Carbon Clusters Revisited: The "Special" Behavior of C60 and Large Carbon Clusters. *J. Chem. Phys.* **1988**, *88*, 1588–1597. DOI: 10.1063/1.454137.

[15] Jones, R. O. Density Functional Study of Carbon Clusters C2n ($2 \leq n \leq 16$). I. Structure and Bonding in the Neutral Clusters. *J. Chem. Phys.* **1999**, *110*, 5189–5200. DOI: 10.1063/1.478414.

[16] Strout, D. L.; Scuseria, G. E. A Cycloaddition Model for Fullerene Formation. *J. Phys. Chem.* **1996**, *100*, 6492–6498. DOI: 10.1021/jp9530212.

[17] Churilov, G. N.; Novikov, P. V.; Tarabanko, V. E.; Lopatin, V. A.; Vnukova, N. G.; Bulina, N. V. On the Mechanism of Fullerene Formation in a Carbon Plasma. *Carbon* **2002**, *40*, 891–896. DOI: 10.1016/S0008-6223(01)00211-1.

[18] Smirnov, B. M. Cluster Plasma. Phys.-*Usp.* **2000**, *43*, 453–491. DOI: 10.1070/PU2000v043n05ABEH000722.

[19] Mitchner, M.; Kruger, C. H. *Partially Ionized Gases*; John Willey & Sons: NY, **1973**.

[20] Kresse, G.; Furthmüller, J. Efficient Iterative Schemes for *Ab Initio* Total-Energy Calculations Using a Plane-Wave Basis Set. *Phys. Rev. B.* **1996**, *54*, 11169–11186. DOI: 10.1103/PhysRevB.54.11169.

[21] Zeiri, Y.; Redondo, A.; Goddard, W. A. III, Classical Stochastic Diffusion Theory for Desorption from Solid Surfaces. *Surf. Sci.* **1983**, *131*, 221–238. DOI: 10.1016/0039-6028(83)90129-2.

[22] Abramovich, G. N. *The Theory of Turbulent Jets*; Schindel, L., Ed. MIT Press: Cambridge, MA, **2003**.